Bisubstrate Inhibition: Theory and Application to *N*-Acetyltransferases†

Michael Yu,‡ Maria L. B. Magalhães,‡ Paul F. Cook,*,§ and John S. Blanchard*,‡

Department of Biochemistry, Albert Einstein College of Medicine, 1300 Morris Park Avenue, Bronx, New York 10461, and Department of Chemistry and Biochemistry, University of Oklahoma, 620 Parrington Oval, Norman, Oklahoma 73019

Received August 9, 2006; Revised Manuscript Received September 20, 2006

ABSTRACT: Bisubstrate inhibitors represent a potentially powerful group of compounds that have found significant therapeutic utility. Although these compounds have been synthesized and tested against a number of enzymes that catalyze sequential bireactant reactions, the detailed theory for predicting the expected patterns of inhibition against the two substrates for various bireactant kinetic mechanisms has, heretofore, not been presented. We have derived the rate equations for all likely sequential bireactant mechanisms and provide two examples in which bisubstrate inhibitors allow the kinetic mechanism to be determined. Bisubstrate inhibitor kinetics is a powerful diagnostic for the determination of kinetic mechanisms.

Enzymes that have two substrates and catalyze their reaction via initial ternary complex formation, followed by chemical steps and product release, are by far the most numerous in biological systems. These include kinases, dehydrogenases and reductases, glycosyl-, methyl-, acetyl-, succinyl-, myristoyl-, palmitoyl-, farnesyl- and geranyltransferses to name just a few. The vast majority of these bireactant mechanisms are catalyzed via sequential kinetic mechanisms in which the binding of the two substrates can be ordered or random, as distinguished from ping-pong kinetic mechanisms typified by PLP-dependent amino transferases and flavin-dependent oxidoreductases. In addition, there are sequential bireactant segments in ter-reactant mechanisms, including those reactions catalyzed by amino acyl-tRNA synthetases and other synthetases and ligases, where activation of one substrate is accomplished by the formation of an activated (often adenylylated or phosphorylated) enzyme-bound intermediate that reacts subsequently with a third substrate. All of these varied reactions have, and can be, probed by the design of bisubstrate analogue inhibitors.

The covalent coupling of two substrates can potentially increase the affinity of the "bisubstrate" by the product of the two association constants of those substrates. This is rarely achieved, since covalent mimics of a transition state cannot be chemically attained. However, this has not prevented the use of bisubstrate analogues as biochemical and structural probes of mechanism and, in a surprising number of cases, has led to the development of compounds with powerful therapeutic properties. Mupirocin (pseudomonic acid-A) is a femtomolar inhibitor of bacterial isoleucyl-tRNA synthetase and is the most widely used topical antibiotic (*1*). Fluorodeoxyuridine monophosphate (FdUMP) is widely used to treat human proliferative disorders. This molecule forms a covalently linked bisubstrate analogue after chemistry is initiated by thymidylate synthase (*2*). Finally, isoniazid (isonicotinic acid hydrazide) is a pro-drug used in the prophylaxis and treatment of tuberculosis. It is oxidized by the mycobacterial *katG*-encoded catalase-peroxidase, generating an isonicotinoyl radical that reacts with NAD^+ and $NADP^+$ to form the 4-isonicotinoyl adducts that are nanomolar, bisubstrate inhibitors of the *Mycobacterium tuberculosis* enoyl-ACP reductase (InhA) (*3*) and dihydrofolate reductase (DHFR) (*4*), respectively.

Bisubstrate inhibitors have been particularly useful in studies of the Gcn5-related *N*-acetyltransferase (GNAT) superfamily. One of the very first examples of such a designed bisubstrate analogue was the synthesis of a gentamicin-acetylCoA and the demonstration that it inhibited the gentamicin *N*-acetyltransferase with nanomolar affinity (*5*). More recently, AuClair and co-workers have generated a series of 6′-*N*-acetylCoA bisubstrate analogues with nanomolar affinity for the *Enterococcus faecalis aac(6′)*-Iy-encoded aminoglycoside 6′-*N*-acetyltransferase (*6*). Cole and co-workers similarly prepared a bisubstrate analogue of tryptamine-acetylCoA and demonstrated that this compound bound to serotonin *N*-acetyltransferase with nanomolar affinity (*7*). The bisubstrate analogue exhibited competitive inhibition versus acetylCoA (AcCoA; K_i = 90 nM) and noncompetitive inhibition versus tryptamine. This compound was also cocrystallized with the enzyme, allowing for specific residues involved in binding and catalysis to be assessed (*8*). Finally, bisubstrate peptidylCoA analogues have been synthesized and shown to inhibit the *Tetrahymena* Gcn5 (tGcn5) histone acetyltransferase at submicromolar levels (*9*). In this latter case, the N-terminal 20-amino acid sequence of histone H3 was linked to CoA via stable ϵ-lysyl−amide and coenzyme A−thioether linkages, and the cocrystallization of the bisubstrate analogue with the enzyme revealed details of substrate binding and catalytic function.

Despite more than 30 years of development and use, the utility of bisubstrate analogues as a diagnostic for kinetic

† This work was supported by NIH Grants AI 60899 (to J.S.B.) and GM 71417 (to P.F.C.) and T32 GM07288 (to M.Y.).

* To whom correspondence should be addressed. J.S.B.: phone, (718) 430-3096; fax, (718) 430-8565; e-mail, blanchar@aecom.yu.edu. P.F.C.: phone, (405) 325-4581; fax, (405) 325-7182; e-mail, pcook@chemdept.chem.ou.edu.

‡ Albert Einstein College of Medicine.

§ University of Oklahoma.

10.1021/bi061621t CCC: $33.50
Published on Web 11/15/2006

mechanisms has not been described in detail. Here we present a theoretical analysis of bisubstrate inhibition for enzymes catalyzing both random and ordered kinetic mechanisms. The theory is borne out experimentally in two such systems.

THEORY

Bisubstrate Analogue Dead-End Inhibition Studies. The treatment of the kinetics of bisubstrate analogue inhibitors was briefly discussed by Fromm (*10*) and Cleland (*11*). Given the interest in the synthesis and analysis of these compounds, we have developed theory and present equations for inhibition by freely reversible bisubstrate analogues in bireactant mechanisms. The ordered and random cases are considered, steady-state equations developed, and the expressions for the intrinsic K_i of the inhibitor presented. To assess the inhibition pattern, the initial rate is measured with one reactant concentration fixed equal to its K_m (unless otherwise specified) and the level of the other reactant varied at different fixed concentrations of the inhibitor, including zero.

Consider an ordered bi-bi reaction mechanism for which a bisubstrate analogue, I_{A-B}, is a mimic of both reactants, i.e., functionally contains both reactants, or structural analogues of the reactants, covalently linked to one another. In the simplest and likely the most frequently observed case, I_{A-B} will bind only to E as shown in Scheme 1.

Scheme 1

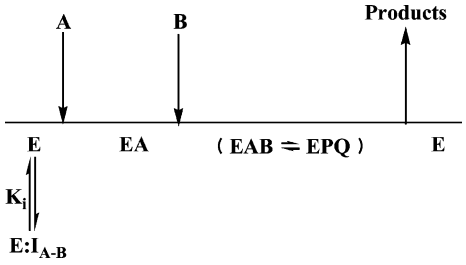

Once bound, the analogue occupies the A and B subsites of the active site and precludes binding of either A or B. In the case of the mechanism shown as Scheme 1, I_{A-B} will compete with A for E, but B can still bind to EA. As a result, increasing the level of B will eliminate some of the inhibition because it increases the competitiveness of A by trapping EA in EAB, and/or complexes downstream, from which A cannot escape. If the mechanism is equilibrium ordered, inhibition can be completely eliminated as the concentration of B increases and all enzyme is forced into central complexes. The rate equation for the steady-state ordered case is given below and is derived from the rate equation in the absence of inhibitor (*12*) by multiplying the terms representing E in the denominator of the rate equation by $1 + [I_{A-B}]/K_i$.

$$v = \frac{V[A][B]}{(K_{ia}K_b + K_a[B])\left(1 + \frac{[I_{A-B}]}{K_i}\right) + K_b[A] + [A][B]} \quad (1)$$

With A as the varied substrate, only the slope of the double-reciprocal plot is affected.

$$\frac{1}{v} = \left(\frac{K_{ia}K_b}{V[B]} + \frac{K_a}{V}\right)\left(1 + \frac{[I_{A-B}]}{K_i}\right)\left(\frac{1}{[A]}\right) + \frac{K_b}{V[B]} + \frac{1}{V} \quad (2)$$

An appK_i is obtained from the slope replot (slope vs 1/[B]) and is defined as the value of $[I_{A-B}]$ when the slope is equal to zero. From eq 2

$$\text{app}K_i = K_i \quad (3)$$

With B varied, both the slope and the intercept of a plot of $1/v$ versus 1/[B] are affected by I_{A-B} and the inhibition is noncompetitive. Expressions for appK_i, obtained from the slope and intercept replots as a function of [A], as discussed above, give eqs 4 and 5, respectively.

$$\text{app}K_i = K_i\left(1 + \frac{[A]}{K_{ia}}\right) \quad (4)$$

$$\text{app}K_i = K_i\left(1 + \frac{[A]}{K_a}\right) \quad (5)$$

If the mechanism is equilibrium-ordered, the rate equation is

$$v = \frac{V[A][B]}{K_{ia}K_b\left(1 + \frac{[I_{A-B}]}{K_i}\right) + K_b[A] + [A][B]} \quad (6)$$

and I_{A-B} is competitive versus both A and B. With A varied, the appK_i is equal to K_i, while if B is varied, app$K_i = K_i(1 + [A]/K_a)$. This mechanism can be distinguished from the random mechanism discussed below since the primary plot with [B] varied at different fixed concentrations of A, in the absence of inhibitors, will intersect on the ordinate.

The random mechanism will behave like the equilibrium ordered mechanism but gives primary plots that intersect to the left of the ordinate whatever substrate is varied. As for the ordered mechanisms, I_{A-B} can combine only with E (Scheme 2).

Scheme 2

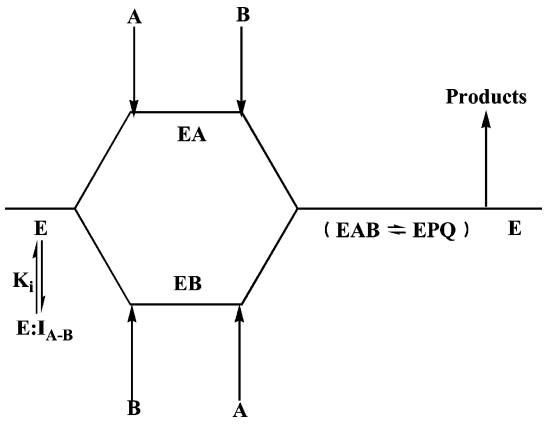

In most cases, the rate equation adheres to the equilibrium random case given in eq 7.

$$v = \frac{V[A][B]}{K_{ia}K_b\left(1 + \frac{[I_{A-B}]}{K_i}\right) + K_a[B] + K_b[A] + [A][B]} \quad (7)$$

In this case, I_{A-B} will be competitive against both reactants since either can bind to E. The expressions for appK_i with A and B varied are as follows: app$K_i = K_i(1 + K_a[B]/K_{ia}K_b)$ and app$K_i = K_i(1 + [A]/K_{ia})$, respectively. When the mechanism is rapid equilibrium, $K_{ia}K_b = K_aK_{ib}$, and when A is varied, app$K_i = K_i(1 + [B]/K_{ib})$.

Caveats. The bisubstrate analogue, I_{A-B}, contains structural mimics of both A and B and thus can also bind to the B subsite in the EA complex in an ordered mechanism. In this case, Scheme 3 is obtained:

Scheme 3

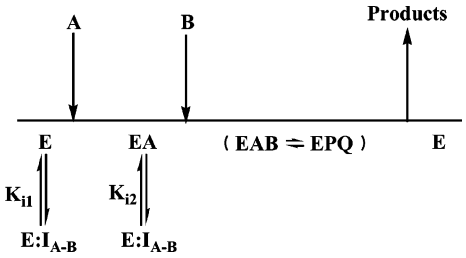

and eq 1 is modified to give eq 8.

$$v = \frac{V[A][B]}{(K_{ia}K_b + K_a[B])\left(1 + \frac{[I_{A-B}]}{K_{i1}}\right) + (K_b[A])\left(1 + \frac{[I_{A-B}]}{K_{i2}}\right) + [A][B]} \quad (8)$$

The inhibition by I_{A-B} is now noncompetitive versus both A and B. When A is bound, the affinity of enzyme for the bisubstrate analogue will be much lower, i.e., $K_{i1} < K_{i2}$. In this case, if A is varied, the expressions for appK_i obtained from slope and intercept terms are given by eqs 9 and 10.

$$\text{app}K_i = K_{i1} \quad (9)$$

$$\text{app}K_i = K_{i2}\left(1 + \frac{K_b}{[B]}\right) \quad (10)$$

With B varied, however, the following expressions are obtained from the slope and intercept replots.

$$\text{app}K_i = \frac{1 + \frac{[A]}{K_{ia}}}{\frac{1}{K_{i1}} + \frac{[A]}{K_{ia}K_{i2}}} \quad (11)$$

$$\text{app}K_i = K_{i1}\left(1 + \frac{[A]}{K_a}\right) \quad (12)$$

The limits of eq 11 indicate that when $[A] < K_{ia}$, app$K_i = K_{i1}$, while if $[A] > K_{ia}$, app$K_i = K_{i2}$.

If the mechanism approximates the Theorell−Chance system (Scheme 4), the release of Q limits the overall reaction, and EQ builds up at saturating reactant concentrations.

Scheme 4

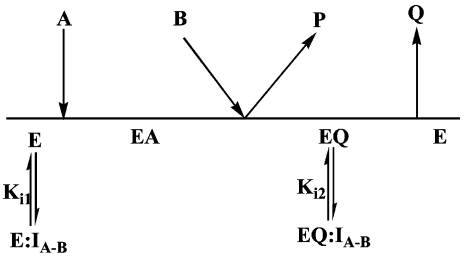

With A or B as the varied substrate, the inhibition will be noncompetitive if there is sufficient affinity of I_{A-B} for the EQ complex. The rate equation in this case is given below.

$$v = \frac{V[A][B]}{(K_{ia}K_b + K_a[B])\left(1 + \frac{[I_{A-B}]}{K_{i1}}\right) + K_b[A] + [A][B]\left(1 + \frac{[I_{A-B}]}{K_{i2}}\right)} \quad (13)$$

In a process similar to Scheme 4, since Q is bound, the affinity of the enzyme for the inhibitory analogue will be much lower, i.e., $K_{i1} < K_{i2}$. If A is varied, the expressions for appK_i obtained from slope and intercept terms are given by eqs 9 and 10. With B varied, the appK_i obtained from the slope is given by eq 4, while the intercept expression is given in eq 14.

$$\text{app}K_i = \frac{1 + \frac{K_a}{[A]}}{\frac{1}{K_{i2}} + \frac{K_a}{[A]K_{i1}}} \quad (14)$$

The limits of eq 14 indicate that when $[A] > K_a$, app$K_i = K_{i2}$, while if $[A] < K_{ia}$, app$K_i = K_{i1}$. Binding of the product AMP-tobramycin, essentially a bisubstrate analogue, to the E−AMP-tobramycin complex of the aminoglycoside nucleotidyltransferase 2″-I was observed by Northrop (*13*), which supports a mechanism that approximates the Theorell−Chance system.

In the case of the random mechanism, it is possible for I_{A-B} to bind to EA (B subsite) and/or EB (A subsite). Thus, noncompetitive inhibition is observed by I_{A-B} whether A or B is varied. Again, if these complexes form, the K_i values will be much greater than those for binding to E. Scheme 5 is applicable in this case.

The initial rate equation is given by eq 15.

Scheme 5

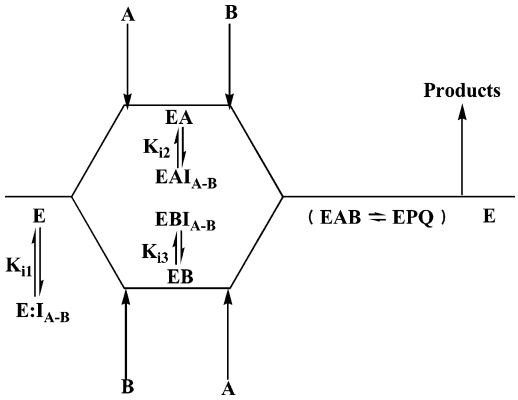

$$v = \frac{V[A][B]}{K_{ia}K_b\left(1 + \frac{[I_{A-B}]}{K_{i1}}\right) + K_a[B]\left(1 + \frac{[I_{A-B}]}{K_{i2}}\right) + K_b[A]\left(1 + \frac{[I_{A-B}]}{K_{i3}}\right) + [A][B]} \quad (15)$$

With A as the varied reactant, expressions for appK_i obtained from the slope and intercept are given in eqs 16 and 17.

$$\text{app}K_i = \frac{1 + \frac{K_a[B]}{K_{ia}K_b}}{\frac{1}{K_{i1}} + \frac{K_a[B]}{K_{ia}K_bK_{i2}}} \quad (16)$$

$$\text{app}K_i = K_{i3}\left(1 + \frac{[B]}{K_b}\right) \quad (17)$$

Limits to eq 16 indicate that that when $[B] < K_{ia}K_b/K_a$, app$K_i = K_{i1}$, while if $[B] > K_{ia}K_b/K_a$, app$K_i = K_{i2}$.

Since the mechanism is symmetric with respect to inhibition by I_{A-B}, the expressions obtained for appK_i when B is varied are qualitatively identical to eqs 16 and 17, as shown in eqs 18 and 19, respectively.

$$\text{app}K_i = \frac{1 + \frac{[A]}{K_{ia}}}{\frac{1}{K_{i1}} + \frac{[A]}{K_{ia}K_{i3}}} \quad (18)$$

$$\text{app}K_i = K_{i2}\left(1 + \frac{[A]}{K_a}\right) \quad (19)$$

Limits to eq 18 are similar to those of eq 16, with the exception that K_{i3} replaces K_{i2}.

If only the EAI_{A-B} or the EBI_{A-B} complex forms, the K_{i2} or K_{i3} terms would be eliminated from eqs 15−19. If EAI_{A-B} is absent, inhibition would be competitive versus A and noncompetitive versus B, while the opposite is true if EBI_{A-B} is absent.

Limitations. In the simplest case, competitive inhibition versus both reactants is diagnostic for a random mechanism with no EAI_{A-B} or the EBI_{A-B} complexes, for example, binding only to E. If a competitive pattern is observed versus one reactant and a noncompetitive pattern is observed versus the other, the simple ordered mechanism cannot be distinguished from a random mechanism with one dead-end ternary complex, and the diagnosis must rely on the quantitative analysis since $K_{i1} < K_{i2}$ and K_{i3}. If noncompetitive inhibition is observed versus both reactants, discrimination between the ordered mechanism with a dead-end EAI_{A-B} complex and a random mechanism with EAI_{A-B} and the EBI_{A-B} complexes will not be possible unless there is a significant difference between K_{i2} (EAI_{A-B}) and K_{i3} (EBI_{A-B}). The random mechanism with EAI_{A-B} and the EBI_{A-B} complexes is the least likely to be encountered.

MATERIALS AND METHODS

Synthesis of ChloroacetylCoA. One equivalent of coenzyme A hydrate (Sigma), 3 equiv of chloroacetic anhydride, and 5 equiv of triethylamine were added to prechilled DMF. The reaction was allowed to proceed for 50 min. The completion of the reaction was monitored by the disappearance of the CoA thiol using DTNB. One milliliter of water was added at the completion of the reaction, and the mixture was lyophilized. ChloroacetylCoA (ClAcCoA) was purified by high-pressure liquid chromatography (HPLC) on a 250 mm × 10 mm Phenomenex Synergi Fusion reverse phase C18 column with a 80 min linear gradient from 0 to 100% methanol at 4 mL/min containing 0.2% aqueous trifluoroacetic acid (TFA). The retention times of CoA and ClAcCoA were 27 and 39 min, respectively.

Synthesis of 3-Tobramycin-AcetylCoA. The regioselective 3-chloroacetylation of tobramycin by AAC(3)-IV was performed using 250 μM ClAcCoA, 200 μM tobramycin, 50 mM K_2HPO_4 (pH 7.0), and 2 μM AAC(3)-IV at room temperature for 1 h. CoA (1.5 mM) was added, and 200 mM Tris (pH 8.4) was used to increase the pH of the solution that was allowed to stand at 4 °C overnight. The following morning, the pH value was adjusted to 2 by adding TFA. After the precipitated AAC(3)-IV had been removed by centrifugation, tobramycin was separated from CoA and 3-tobramycin-acetylCoA by HPLC using a Phenomenex Synergi Fusion reverse phase C18 column (4 μm, 250 mm × 21.2 mm) using an 80 min linear gradient from 0.5 to 35% acetonitrile containing 0.1% TFA at a rate of 8 mL/min. The retention time of tobramycin was 17 min, while the retention times of CoA and 3-tobramycin-acetylCoA were 31 min. Fractions containing CoA and 3-tobramycin-acetylCoA were lypophilized after acetonitrile was removed by rotary evaporation. CoA and 3-tobramycin-acetylCoA were dissolved in 20 mM sodium acetate (pH 5.5) and loaded onto a 10 mL Mono Q (Amersham) column preequilibrated with 10 mM sodium acetate (pH 5.5). CoA and 3-tobramycin-acetylCoA were eluted with a linear gradient of buffer A [10 mM sodium acetate (pH 5.5)] to buffer B [1 N NaCl and 50 mM sodium acetate (pH 5.5)] over 1 h at a rate of 1 mL/min. 3-Tobramycin-acetylCoA and CoA were eluted at 20 and 60 min, respectively. Tobramycin-CoA was desalted by binding and elution from a Phenomenex Synergi Fusion Rp C18 column using the gradient described above. The yield of 3-tobramycin-acetylCoA is 30%, and the identity of the product was confirmed by mass spectrometry.

Synthesis of $S18_{1-6}$-AcetylCoA. The chloroacetylation of the six N-terminal amino acids of ribosomal protein S18 was

performed using 300 μM ClAcCoA, 300 μM $S18_{1-6}$ peptide (ARYFRR), 50 mM K_2HPO_4 (pH 7.0), and 5 μM RimI at room temperature for 1 h. CoA (1.5 mM) was added, and 200 mM Tris (pH 8.4) was used to increase the pH of the solution that was allowed to stand at 4 °C. After 10 h, TFA was added to the reaction mixture. After the precipitated RimI had been removed via centrifugation, the $S18_{1-6}$-acetylCoA peptide was separated from CoA and $S18_{1-6}$ peptide by HPLC using a Phenomenex Synergi Fusion reverse phase C18 column (4 μm, 250 mm × 21.2 mm) using a linear gradient from 0 to 35% acetonitrile containing 0.1% TFA over 60 min at a rate of 10 mL/min. The retention times of CoA, $S18_{1-6}$ peptide, and CoAylated $S18_{1-6}$ were 23, 33, and 40 min, respectively. The yield of $S18_{1-6}$-acetylCoA is 25%, and the identity of the product was confirmed by mass spectrometry.

Enzyme Assays. AAC(3)-IV from *Escherichia coli* was purified as described previously (*14*). Aminoglycoside-dependent acetyltransferase activity was monitored spectrophotometrically by following the increase in absorbance at 324 nm due to the reaction between the sulfhydryl group of the product CoASH and 4,4′-dithiodipyridine (DTDP), releasing 4-thiopyridone (ϵ_{324} = 19 800 M^{-1} cm^{-1}). Reactions were monitored continuously on a UVIKON XL spectrophotometer, and enzyme activities were calculated from the initial (<10% completion) rates. Assay mixtures contained 50 mM HEPES (pH 7.5) and 0.1 mM DTDP, in addition to enzyme, substrate, and inhibitors in a final volume of 1 mL. Reactions were initiated by the addition of enzyme and followed at 25 °C.

Reaction rates of the RimI-catalyzed acetylation of $S18_{1-6}$ were determined by continuously monitoring the increase in absorbance at 412 nM due to the formation of 5-thio-2-nitrobenzoate resulting from the reaction between the sulfhydryl group of the product, CoA-SH, and 5,5′-dithiobis(2-nitrobenzoic acid) (DTNB) (ϵ_{412} = 13 600 M^{-1}). Assays were performed at 25 °C in 50 mM KH_2PO4 (pH 7.25) containing 100 μM DTNB as described above. Inhibition patterns were determined by measuring initial velocities at variable concentrations of one reactant and at a fixed concentration of the second reactant, where the fixed AcCoA concentration was 1.8 μM and the fixed $S18_{1-6}$ concentration was 1 mM.

Bisubstrate Analogue Inhibition Patterns. Bisubstrate inhibition patterns for 3-tobramycin-acetylCoA were determined by measuring initial velocities at five different concentrations of one reactant, a fixed concentration of the second reactant, and different concentrations of the bisubstrate analogue. First, the tobramycin concentration was varied (4, 5, 6.6, 10, and 20 μM), and the acetylCoA concentration was held at 60 μM. Four different concentrations of 3-tobramycin-acetylCoA were tested (0, 50, 100, and 150 nM), and the data were fitted to eqs 20 and 21, which describe linear competitive and noncompetitive inhibition, respectively.

$$v = V[A]/[K_a(1 + [I_{A-B}]/K_{is})] \quad (20)$$

$$v = V[A]/[K_a(1 + [I_{A-B}]/K_{is}) + [A](1 + [I_{A-B}]/K_{ii})] \quad (21)$$

where v is the measured reaction velocity, V is the maximal velocity, [A] is the concentration of the varied substrate, K_a is the corresponding Michaelis−Menten constant, $[I_{A-B}]$ is the concentration of bisubstrate inhibitor, and K_{is} and K_{ii} are the slope and intercept inhibition constants, respectively. Analogous experiments were performed using RimI, the $S18_{1-6}$ peptide substrate, and the $S18_{1-6}$-acetylCoA bisubstrate analogue.

Bisubstrate inhibition patterns were also determined by varying the acetylCoA concentration (50, 65, 85, 130, and 260 μM) using tobramycin at a fixed concentration of 2 μM. Five different concentrations of 3-tobramycin-acetylCoA were tested (0, 12.5, 25, 37.5, and 50 nM), and the data were fitted to eq 18.

Determination of the True K_i Value. To determine the true K_i value for 3-tobramycin-acetylCoA, appK_i values were determined from individual double-reciprocal plots using five different concentrations of the nonvaried reactant (tobramycin at 2, 4, 6, 8, and 10 μM).

The appK_i values were plotted against the concentration of tobramycin, and the data were fitted to the equation appK_i = $K_i(1 + [B]/K_{ib})$, where K_i is the true inhibition constant for 3-tobramycin-acetylCoA, appK_i is the apparent inhibition constant, [B] is the concentration of the nonvaried substrate (tobramycin), and K_{ib} is the dissociation constant for substrate B.

The entire data set was also fitted to eq 7, which describes equilibrium random cases where neither EAI_{A-B} nor EBI_{A-B} forms, where v is the measured reaction velocity, V is the maximal velocity, [A] and [B] are the concentrations of substrates A and B, respectively, K_a and K_b are the corresponding Michaelis−Menten constants, K_{ia} is the dissociation constant for substrate A, $[I_{A-B}]$ is the concentration of the bisubstrate analogue, and K_i is the inhibition constant for the bisubstrate analogue.

RESULTS AND DISCUSSION

Inhibition Studies of RimI. A kinetic mechanism has been established for RimI that involves transfer of the acetyl group from AcCoA to $S18_{1-6}$ peptide via a sequential mechanism (M. W. Vetting et al., unpublished data). The initial velocity pattern of the reciprocal $S18_{1-6}$ concentration at different fixed concentrations of AcCoA resulted in an intersecting initial velocity pattern, where the determined kinetic parameters are as follows: k_{cat} = 19 ± 1 min^{-1}, K_{AcCoA} = 0.35 ± 0.08 μM, and $K_{S18_{1-6}}$ = 2.2 ± 0.2 mM (data not shown). We used the bisubstrate inhibitor, $S18_{1-6}$-acetylCoA, to differentiate between random and ordered mechanisms. The bisubstrate inhibitor is linearly competitive versus acetylCoA and linearly noncompetitive versus $S18_{1-6}$ as evidenced by E/v versus 1/[AcCoA] and E/v versus 1/$[S18_{1-6}]$ intersecting on and to the left of the y-axis, respectively (Figure 1). The apparent K_i value determined from the competitive pattern versus AcCoA (4.1 ± 0.4 μM) is equivalent to the slope and intercept inhibition constants determined from the noncompetitive pattern observed for the bisubstrate versus $S18_{1-6}$ (K_{is} = 12 ± 1 μM and K_{ii} = 8.2 ± 0.8 μM). RimI thus follows an ordered kinetic mechanism, where AcCoA binds first to the free enzyme followed by the peptide substrate $S18_{1-6}$, without significant accumulation of an EAI_{A-B} complex. This pattern was previously observed for

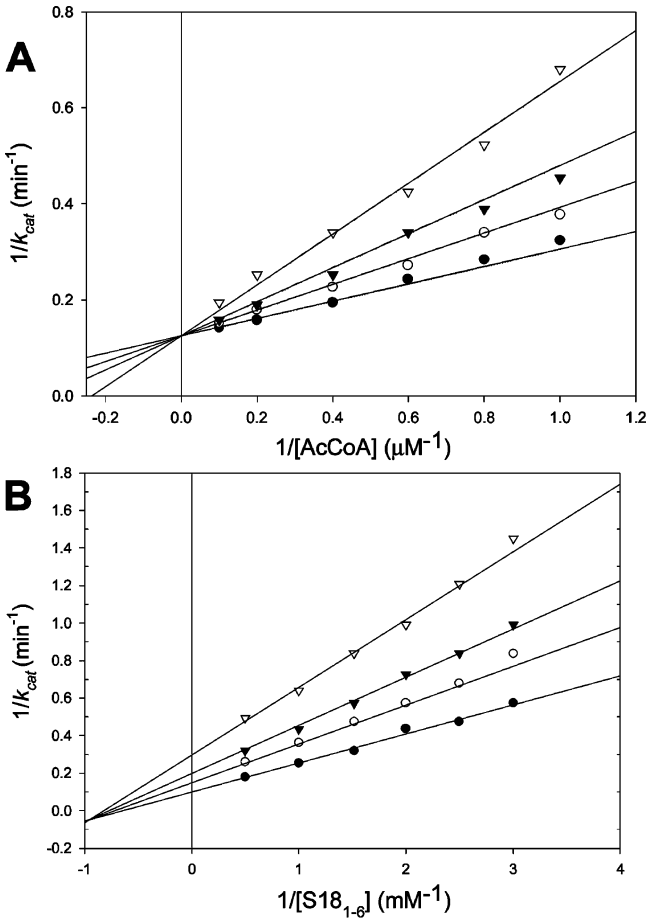

FIGURE 1: Bisubstrate inhibition studies of RimI. (A) Plot of $1/k_{cat}$ vs 1/[AcCoA] at varying concentrations of the $S18_{1-6}$-acetylCoA inhibitor and a fixed $S18_{1-6}$ concentration of 1 mM. The symbols represent the experimentally determined values, whereas the solid lines are the best fit of the data to eq 20. V_{max} (8.0 ± 0.2 min^{-1}), apparent K_{AcCoA} (1.4 ± 0.1 μM), and K_{is} (4.1 ± 0.4 μM) are the fitted parameters. The bisubstrate inhibitor was varied [(▽) 8, (▼) 4, (○) 2, and (●) 0 μM] at fixed levels (1, 1.25, 1.67, 2.5, 5, and 10 μM) of AcCoA. (B) Plot of $1/k_{cat}$ vs 1/[$S18_{1-6}$] at varying concentrations of $S18_{1-6}$-acetylCoA inhibitor and 1 μM AcCoA. The symbols represent the experimentally determined values, whereas the solid lines are the best fit of the data to eq 21. V_{max} (9.9 ± 0.3 min^{-1}), apparent $K_{S18_{1-6}}$ (1.5 ± 0.1 mM), K_{is} (12 ± 1.0 μM), and K_{ii} (8.2 ± 0.8 μM) are the determined parameters. The inhibitor concentration was varied [(▽) 16, (▼) 8, (○) 4, and (●) 0 μM] at fixed levels (0.33, 0.4, 0.5, 0.67, 1, and 2 mM) of $S18_{1-6}$.

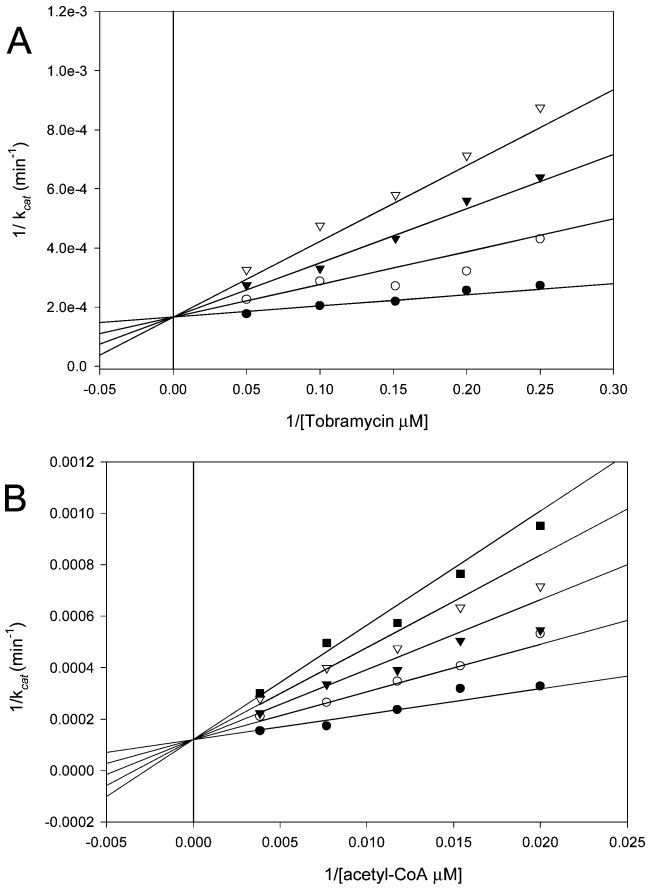

FIGURE 2: Bisubstrate inhibition studies of AAC(3)-IV. (A) Plot of $1/k_{cat}$ vs 1/[tobramycin] at varying concentrations of 3-tobramycin-acetylCoA inhibitor [(▽) 150, (▼) 100, (○) 50, and (●) 0 nM] and a fixed AcCoA concentration of 60 μM. The symbols represent the experimentally determined values, whereas the solid lines are the best fit of the data to eq 18. (B) Plot of $1/k_{cat}$ vs 1/[AcCoA] at varying concentrations of 3-tobramycin-acetylCoA inhibitor [(■) 50, (▽) 37.5, (▼) 25, (○) 12.5, and (●) 0 nM] and a fixed tobramycin concentration of 2 μM. The symbols represent the experimentally determined values, whereas the solid lines are the best fit of the data to eq 20.

the tryptamine-acetylCoA bisubstrate inhibitor of serotonin *N*-acetyltransferase (*7*) and was used to support an ordered addition of substrates. The subsequent structural characterization of the apoenzyme and complexes of the enzyme with substrates, and the bisubstrate analogue, revealed large conformational changes associated with the binding of acetylCoA that serve to "build" the tryptamine/serotonin binding site, including the orientation of active site residues thought to participate in catalysis (*8*).

Inhibition Studies with AAC(3)-IV. The *E. coli* AAC(3)-IV aminoglycoside-modifying enzyme was first isolated from veterinary isolates that were resistant to gentamicin (*15*). The enzyme exhibits broad substrate specificity for both 4,5- and 4,6-disubstituted deoxystreptamine aminoglycosides, as well as activity with the atypical aminoglycoside apramycin, used exclusively for veterinary purposes. The kinetic mechanism has been proposed to be random, on the basis of the observed patterns of dead end inhibitors versus substrates and non-Michaelis−Menten behavior of certain aminoglycoside substrates (*14*). Although Auclair was able to chemically generate the 6′-tobramycin-acetylCoA bisubstrate analogue (*6*), the poorer reactivity of the secondary 3-amino group of tobramycin prevents regioselective acetylCoA-ylation. The bisubstrate inhibitor was thus generated enzymatically using AAC(3)-IV, chloroacetylCoA, and tobramycin. The compound exhibited linear competitive inhibition versus both AcCoA and tobramycin (Figure 2A,B). When the apparent K_i value versus AcCoA of the bisubstrate inhibitor was determined at several concentrations of tobramycin, the apparent K_i value decreased as the tobramycin concentration decreased, as expected for an inhibitor that binds to both substrate-binding sites (Figure 3). These data allow the true K_i value for the binding of the bisubstrate to the free enzyme to be determined by extrapolation to 0 mM tobramycin, yielding a value of 11 ± 3 nM.

With the equations for the random case described above, we also fitted all the data obtained for the inhibition of the bisubstrate versus AcCoA at five different tobramycin

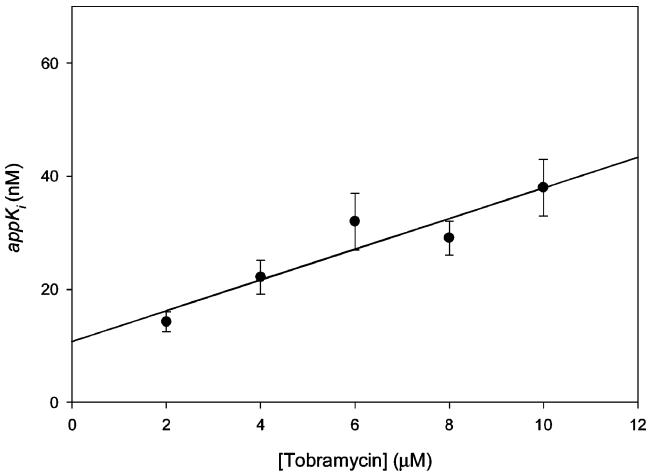

FIGURE 3: Linear dependence of appK_i values at various concentrations of tobramycin. Symbols represent the experimentally determined values, while the solid line is the fit of the data to eq 7, where $K_{ia} = 3.9 \pm 2.2$ μM and $K_i = 11 \pm 3$ nM.

concentrations and fitted these data to eq 7. This "global" fit yielded the following kinetic parameters: $V = 12\,000 \pm 1000$ min^{-1}, $K_{AcCoA} = 68 \pm 16$ μM, $K_{tob} = 0.7 \pm 0.4$ μM, and $K_{i,AcCoA} = 160 \pm 160$ μM and for the bisubstrate inhibitor, $K_i = 6 \pm 3$ nM. These values are in close agreement with those values for the kinetic constants reported previously (*14*), and the K_i value was determined by extrapolation. The close agreement of the K_i values, determined by both extrapolation and using the complete rate equation to fit the entire data set, argues persuasively for a random kinetic mechanism, without significant accumulation of ternary enzyme−substrate−inhibitor complexes.

The use of chloroacetylCoA as a reagent for GNAT-encoded acetyltransferases allows for the rapid and efficient synthesis of bisubstrate inhibitors for functionally characterized members of this superfamily. The chloroacetyltransferase reaction retains its regioselectivity when ClAcCoA is used, and the bisubstrate analogues are bound tightly (<100 nM) in most cases described to date. While such inhibitors have been used for the structural characterization of the GNAT-encoded acetyltransferase superfamily, their use as diagnostic tools of kinetic mechanism has been unappreciated to date. The early treatment of their utility neglected several important kinetic variants. The treatment described here provides a strong theoretical framework that should be broadly applicable to the numerous other sequential bireactant enzyme-catalyzed reactions of biomedical importance.

ACKNOWLEDGMENT

We thank Dr. Argyrides Argyrou for assistance in data fitting.

REFERENCES

1. Brown, M. J. B., Mensah, L. M., Doyle, M. L., Broom, N. J. P., Osborne, N., Forrest, A. K., Richardson, C. M., O'Hanlon, P. J., and Pope, A. J. (2000) Rational Design of Femtomolar Inhibitors of Isoleucyl tRNA Synthetase from a Binding Model for Pseudomonic Acid-A, *Biochemistry 39*, 6003−11.
2. Pogolotti, A. L., Jr., Ivanetich, K. M., Sommer, H., and Santi, D. V. (1976) Thymidylate synthetase: Studies on peptide containing covalently bound 5-fluoro-2′-deoxyuridylate and 5,10-methylene-tetrahydrofolate, *Biochem. Biophys. Res. Commun. 70*, 972−8.
3. Rozwarski, D. A., Grant, G. A., Barton, D. H., Jacons, W. R., Jr., and Sacchettini, J. C. (1998) Modification of the NADH of the isoniazid target (InhA) from *Mycobacterium tuberculosis*, *Science 279*, 98−102.
4. Argyrou, A., Vetting, M. W., Aladegbami, B., and Blanchard, J. S. (2006) *Mycobacterium tuberculosis* Dihydrofolate Reductase is a Target for Isoniazid, *Nat. Struct. Mol. Biol. 13*, 408−13.
5. Williams, J. W., and Northrop, D. B. (1979) Synthesis of a tight-binding, multisubstrate analog inhibitor of gentamicin acetyltransferase I, *J. Antibiot. 32*, 1147−54.
6. Gao, F., Yan, X., Baettig, O. M., Beghuis, A. M., and Auclair, K. (2005) Regio- and Chemoselective 6′-N-derivatization of Aminoglycosides: Bisubstrate Inhibitors as Probes to Study Aminoglycoside 6′-N-Acetyltransferases, *Angew. Chem., Int. Ed. 44*, 6859−62.
7. Khalil, E. M., and Cole, P. A. (1998) A Potent Inhibitor of the Melatonin Rhythm Enzyme, *J. Am. Chem. Soc. 120*, 6195−6.
8. Hickman, A. B., Namboodiri, M. A. A., Klein, D. C., and Dyda, F. (1999) The Structural Basis of Ordered Substrate Binding by Serotonin N-Acetyltransferse: Enzyme Complex at 1.8 Å Resolution with a Bisubstrate Analog, *Cell 97*, 361−9.
9. Poux, A. N., Cebrat, M., Kim, C. M., Cole, P. A., and Marmorstein, R. (2002) Structure of the GCN5 Histone Acetyltransferase Bound to a Bisubstrate Inhibitor, *Proc. Natl. Acad. Sci. U.S.A. 99*, 14065−70.
10. From, H. J. (1977) Use of Competitive Inhibitors to Study Substrate Binding Order, *Methods Enzymol. 63*, 467−86.
11. Cleland, W. W. (1970) in *The Enzymes* (Boyer, P. D., Ed.) 3rd ed., Vol. II, pp 1−65, Academic Press, New York.
12. Cleland, W. W. (1963) The Kinetics of Enzyme-Catalyzed Reactions with Two or More Substrates or Products: I. Nomenclature and Rate Equations, *Biochim. Biophys. Acta 67*, 104−37.
13. Gates, C. A., and Northrop, D. B. (1988) Substrate specificities and structure-activity relationships for the nucleotidylation of antibiotics catalyzed by aminoglycoside nucleotidyltransferase 2″-I, *Biochemistry 27*, 3820−5.
14. Magalhães, M. L. B., and Blanchard, J. S. (2005) The Kinetic Mechanism of AAC(3)-IV Aminoglycoside Acetyltransferase from *Escherichia coli*, *Biochemistry 44*, 16275−83.
15. Chaslus-Dancla, E., Martel, J. L., Carlier, C., Lafont, J. P., and Courvalin, P. (1986) Emergence of aminoglycoside 3-*N*-acetyltransferase IV in *Escherichia coli* and *Salmonella typhimurium* isolated from animals in France, *Antimicrob. Agents Chemother. 29*, 239−43.

BI061621T